World Academy of Science, Engineering and Technology
International Journal of Mechanical and Mechatronics Engineering
Vol:4, No:8, 2010

Thermodynamic Performance Assessment of Steam-Injection Gas-Turbine Systems

Kyoung Hoon Kim and Giman Kim

Abstract**—**The cycles of the steam-injection gas-turbine systems are studied. The analyses of the parametric effects and the optimal operating conditions for the steam-injection gas-turbine (STIG) system and the regenerative steam-injection gas-turbine (RSTIG) system are investigated to ensure the maximum performance. Using the analytic model, the performance parameters of the system such as thermal efficiency, fuel consumption and specific power, and also the optimal operating conditions are evaluated in terms of pressure ratio, steam injection ratio, ambient temperature and turbine inlet temperature (TIT). It is shown that the computational results are presented to have a notable enhancement of thermal efficiency and specific power.

Keywords**—**gas turbine, RSTIG, steam injection, STIG, thermal efficiency.

I. Introduction

IN recent years the humidification of a gas turbine system with water or steam injection is of great important factor to enhance the thermal efficiency and the specific power output of a gas turbine. Moreover the gas turbine humidification has the potential of reduced specific investment cost, decreased formation of nitrogen oxides (NOx) in the combustor, and improved part-load performance compared with combined cycles. The basic idea of gas turbine humidification is that the injected water or steam increases the mass flow rate through the turbine and augments the specific power output. Many different cycles with water or steam injection have been suggested, although only a few have been commercialized [1-3].

Evaporative inlet fogging is a simple, proven and cost effective approach for recovering lost gas performance [4-5]. When the mass fraction of water is in the order of 1%, the process is considered as low-fogging. High-fogging generally denotes higher liquid mass fractions, and droplet evaporation is projected to occur during compression. The energy to sustain evaporation cools the air under compression, reducing the mixture volume and hence the compression power. White and Meacock [6] and Kim and Perez-Blanco [7] studied the wet-compression process employing transient heat and mass transfer analysis of evaporating droplets suspended in the air stream. It was shown [7] that the water injection ratio, compression ratio and droplet initial radius be reported as the significant variables to define the evaporation time. The compressor power could be reduced to 70% of its value for a compression ratio of 25 and an injection ratio of 10% [7]. Perez-Blanco et al. [8] investigated for the general case of evaporatively-cooled compression with high-pressure refrigerants. The performance of gas turbine cycles with wet compression (WCG), and also of wet compression followed by recuperation of residual exhaust heat (RWCG) were studied by Kim and Perez-Blanco [9, 10]. In the RWCG cycle case, the compressor discharge was preheated in a recuperator by the turbine exhaust gas, expecting the high thermal efficiency based on the reduction of the fuel input to reach the given TIT.

STIG systems can enhance the thermal efficiency and specific power with relatively low cost by using heat recovery steam generator (HRSG), which is generating the steam from water being heated by the exhaust gas. When water or steam is injected after compressor outlet, power output at turbine can be increased whereas the compression work maintains nearly constant. Wang and Chiou [11] simulated STIG system with inlet air cooling (IAC) and reported that the system implementing both steam injection and IAC can boost both power output and heat rate remarkably. When the energy of the gas turbine exhaust can be recovered by preheating water or generating steam for injection or preheating the combustion air in a recuperator, the thermal efficiency is raised. In case of a recuperated gas turbine, the added water before the combustor reduces the temperature of the compressed air at the inlet to the recuperator, and then increases the energy recovery rate from the exhaust gas. Bassily [12] and Nishida et al [13] reported that the RSTIG systems can have higher efficiency and lower pressure ratio for the maximum efficiency compared with STIG systems.

In this paper, the comparative potential of the performance of STIG and RSTIG systems are discussed. The characteristics of the STIG and RSTIG systems such as thermal efficiency, specific power and fuel consumption are investigated in terms of the parameters such as pressure ratio, steam injection ratio, ambient temperature and TIT. And also the optimal operating conditions for the maximum thermal efficiency are presented

II. System Analysis

The schematic diagrams of STIG and RSTIG cycles are shown in Fig. 1. In the STIG system, air and fuel are compressed from ambient pressure to combustion pressure. Water at ambient temperature is compressed and enters into HRSG and goes out as steam. In the combustion chamber the steam is injected to the compressed air and fuel and the flame adiabatic temperature is reached at constant pressure. The hot gas is then

K. H. Kim is with School of Mechanical Engineering, Kumoh National Institute of Technology, 1 Yangho, Gumi, Gyeongbuk 730-701, Korea (phone: 82-54-478-7292; fax: 82-54-478-7319; e-mail: khkim@ kumoh.ac.kr).

G. Kim is with School of Mechanical Engineering, Kumoh National Institute of Technology, 1 Yangho, Gumi, Gyeongbuk 730-701, Korea (phone: 82-54-478-7294; fax: 82-54-478-7319; e-mail: giman@ kumoh.ac.kr).

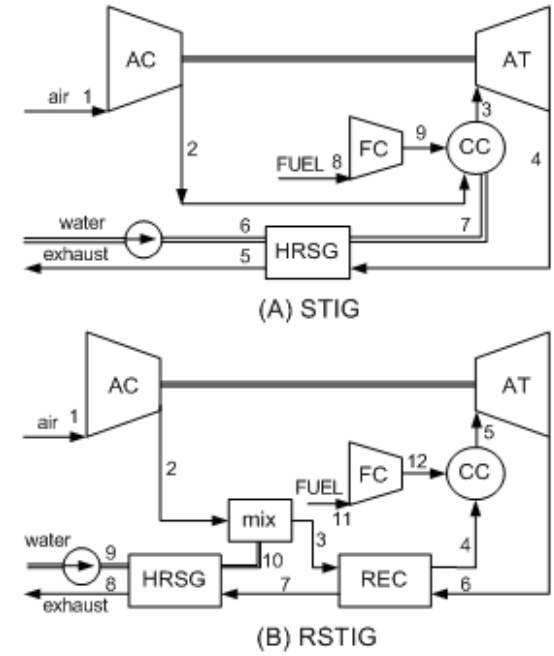

Fig. 1 Schematic diagrams : (A) the steam injection gas turbine (STIG), (B) the regenerative steam injection gas turbine (RSTIG)

expanded and heats the water within HRSG and then is exhausted. In RSTIG systems, liquid and vapor of water produced in the HRSG are mixed with compressor discharge. The exhaust gas at turbine exit is used to preheat the humid air within the recuperator before the air enters into the combustion chamber and also to heat the water within HRSG.

Important assumptions used in this work are as follows.

1) Gases are ideal gases whose thermodynamic properties are varied with temperature.
2) The dry air at compressor inlet consists of 0.2095 moles of O_2, 0.7902 moles of N_2 and 0.0003 moles of CO_2.
3) The fuel is methane (CH_4) and the combustion is complete and adiabatic.
4) Compressors and turbine are characterized with polytropic efficiencies.
5) The effectiveness of recuperator or HRSG is assumed constant.
6) Pressure drop and heat loss of the systems are negligible.

The gases considered in this study are O_2, N_2, CO_2, H_2O and CH_4, which are numbered from 1 to 5 in order. The isobaric specific heat of gas of component *i* can be expressed as

$$c_{p,i} = M_i^{-1} \sum_{j=0}^{3} c_{i,j} T^j \tag{1}$$

where M_i is molecular weight of gas of component *i* and *T* is the temperature in K. By using Eq. (1) enthalpy and entropy function of gas of component *i* can be obtained as

$$h_i(T) = M_i^{-1} \sum_{j=0}^{3} \frac{c_{i,j}}{j+1} T^{j+1} \tag{2}$$

$$s_i^0(T) = M_i^{-1} \left[\bar{s}_i^0 + c_{i,0} \ln\left(\frac{T}{T_{ref}}\right) + \sum_{j=1}^{3} \frac{c_{i,j}}{j} \left(T^j - T_{ref}^j\right) \right] \tag{3}$$

where T_{ref} is the reference temperature of *298.15K* and $\bar{s}_i^0$ means the molar absolute entropy of gas of component *i*. If mass of gas of component *i* per unit mass of dry air is α_i *kg/kg*, moles of the component is denoted as $\gamma_i = \alpha_i / M_i$. Then thermodynamic properties of gas mixture can be expressed as

$$\alpha_m = \sum_{i=1}^{5} \alpha_i \tag{4}$$

$$\gamma_m = \sum_{i=1}^{5} \gamma_i \tag{5}$$

$$M_m = \alpha_m / \gamma_m \tag{6}$$

$$R_m = R_u / M_m \tag{7}$$

$$h(T,\alpha) = \sum_{i=1}^{5} \alpha_i h_i(T) \tag{8}$$

$$s^0(T,\alpha) = \sum_{i=1}^{5} \alpha_i s_i^0(T) \tag{9}$$

$$s(P,T,\alpha) = s^0(T) - \alpha_m R_m \ln\left(P / P_{ref}\right) \tag{10}$$

where α_m, γ_m, M_m, R_m, h, s^0 and s are mass, moles, molecular weight, gas constant, enthalpy, entropy function and entropy of gas mixture, respectively. Enthalpy of liquid water, h_l, can be calculated as

$$h_l(T) = h_4(T) - h_{fg}(T) \tag{11}$$

where h_{fg} is the latent heat of vaporization of water.

Air enters into the compressor at T_1, P_1 and RH_1. All of the computations in this study are based on unit mass of dry air at compressor inlet. Water enters into HRSG at a rate of f_w kg per 1 kg of dry air. For a pressure ratio r_p, the compressor discharge pressure is $P_2 = r_p P_1$. The polytropic efficiencies of compressor and turbine, η_c and η_t are defined as [6-7]:

$$dh = v\,dP / \eta_c \tag{12}$$

$$dh = \eta_t\, v\,dP \tag{13}$$

Here the efficiencies of compressors and turbine are assumed to be decreased linearly with pressure ratio [11, 13]:

$$\eta_c = 1 - \left(0.05 + \frac{r_p - 1}{180}\right) \tag{14}$$

$$\eta_t = 1 - \left(0.10 + \frac{r_p - 1}{180}\right) \tag{15}$$

If the inlet condition of compressor or turbine is specified, the outlet temperature of compressor or turbine can be obtained from the following equations, which reflects the mixture entropy change in the compressor or turbine [7, 9]:

$$s_{out}^0 - s_{in}^0 = \alpha_m R_m \ln\left(r_p\right) / \eta_c \tag{16}$$

$$s_{out}^0 - s_{in}^0 = -\eta_t\, \alpha_m R_m \ln\left(r_p\right) \tag{17}$$

The combustion process can be expressed as [15]

$$CH_4 + 2O_2 \rightarrow CO_2 + 2\,H_2O \tag{18}$$

If mass of fuel per unit mass of dry air is α_f *kg/kg*, mole of fuel becomes as $\gamma_f = \alpha_f / M_f$. From Eq. (18), it is known that mole of CO_2 increases γ_f, mole of H_2O increases $2\gamma_f$, and mole of O_2 decreases $2\gamma_f$ during the combustion process. The fuel

consumption per unit mass of dry air, α_f, can be determined from the following equation [15]:

$$\sum_{i=1}^{5}\alpha_i^r\left[h_i(T_i^r)-h_i(T_{ref})+h_{f,i}^0\right]=\sum_{i=1}^{5}\alpha_i^p\left[h_i(T_i^p)-h_i(T_{ref})+h_{f,i}^0\right] \quad (19)$$

Here subscripts of *r* and *p* denote reactant and production, respectively, and $h_{f,i}^0$ is the enthalpy of formation of component *i*.

The compressor discharge is preheated in the recuperator and water is heated in HRSG. The energy balance over the regenerator or HRSG becomes as

$$h_{h,in}-h_{h,out}=h_{c,out}-h_{c,in} \quad (20)$$

where subscripts h and c denote hot and cold fluid, respectively. The effectiveness of heat exchanger is defined as the ratio of actual heat transfer rate to maximum possible heat transfer rate as [16]:

$$\varepsilon=\frac{q}{q_{\max}} \quad (21)$$

The maximum possible heat transfer rate, $q_{\max}$, is obtained as:

$$q_{\max}=\min\left[h(T_{h,in},\alpha_h)-h(T_{h,in},\alpha_h),h(T_{c,out},\alpha_c)-h(T_{h,in},\alpha_c)\right] \quad (22)$$

III. Results and Discussions

The system parameters used in this work are summarized in Table 1. Typical cases of computations for STIG and RSTIG systems at $T_1 = 15\ ^oC$, $P_1 = 1atm$, $RH_1 = 60\%$, $r_p = 10$, $f_w = 10\%$ are shown in Table 2. Mass flow rates of O_2, N_2, CO_2, and $H_2O(g)$ which are based on unit mass of dry air at compressor inlet are 23.23%, 76.72%, 0.05%, and 1.64%, respectively. After compression T_2 is raised to 338.7°C whereas the mass flow rates of the components are not changed. In the STIG cycle, T_3 at turbine inlet is held at constant value of 1200°C (TIT) and the mass flow rates of components are changed due to combustion as 12.67%, 76.72%, 7.31%, 17.58% in the order of components. T_4 at turbine exit is fallen to 674.5°C and T_5 of exhaust at HRSG exit is 459.1°C. Meanwhile, water at ambient temperature ($T_6 = T_1 = 15$°C) enters into the HRSG and all of them are converted to steam and T_7 at HRSG exit is raised to 372.6°C. The fuel consumption is 2.65% of mass flow rate of dry air.

TABLE I
Calculation Conditions for Gas Turbine Systems

symbol	Parameter	data	unit
T_1	ambient temperature	25	°C
P_1	ambient pressure	101.325	kPa
RH_1	ambient relative humidity	60	%
TIT	turbine inlet temperature	1200	°C
ε	effectiveness of heat exchangers	0.83	
	fuel	CH_4	

In the RSTIG cycle, water of 10% of mass flow rate of dry air at ambient temperature ($T_9 = T_1 = 15$°C) enters into the HRSG, and 9.33% of steam is generated from water and 0.67% is remained as water. Thus, at HRSG exit the working fluid is in the saturated condition and temperature T_{10} is raised to 180.5°C. The air coming out from the compressor is mixed with the two-phase mixture from HRSG in the mixer and T_3 at recuperator inlet is fallen to 304.0°C. At turbine inlet T_5 is held at constant value of 1200 °C (TIT), too and the mass flow rates are changed due to combustion as 15.77%, 76.72%, 5.18%, 11.64% in the order of components. At turbine exit T_6 is fallen to 669.7 °C, and T_7 at recuperator exit and T_8 at HRSG exit are fallen to 383.8°C, and 188.1°C successively. The fuel consumption is 1.87% of mass flow rate of dry air.

In Fig. 2, the thermal efficiency is plotted versus the pressure ratio for various steam injection ratio. In both STIG and RSTIG systems the thermal efficiency increases with pressure ratio up to its maximum value and then subsequently decreases. The thermal efficiency of RSTIG is greater than that of STIG except at high pressure ratios. The optimum pressure ratio at which the maximum thermal efficiency occurs shifts to the right and upwards with increasing injection ratios, and the optimum pressure ratio in STIG is greater than that in RSTIG. In each system thermal efficiency increases with pressure ratio. However in RSTIG, it may not be possible to operate in the range of

TABLE II
Typical Computational Results for $T_1 = 15$°C, $P_1 = 1$atm, $RH_1 = 60\%$, $R_P = 10$, $F_W = 10\%$

position	O_2 (%)	N_2 (%)	CO_2 (%)	$H_2O(g)$ (%)	CH_4 (%)	$H_2O(l)$ (%)	T (°C)	P (kPa)	h (kJ/kg)	s (kJ/kgK)
STIG1	23.23	76.72	0.05	1.64	0.00	0.00	15.0	101.3	294.1	6.87
2	23.23	76.72	0.05	1.64	0.00	0.00	338.7	1013.3	639.6	6.99
3	12.67	76.72	7.31	17.58	0.00	0.00	1200.0	1013.3	2119.6	9.73
4	12.67	76.72	7.31	17.58	0.00	0.00	674.5	101.3	1287.7	9.85
5	12.67	76.72	7.31	17.58	0.00	0.00	459.1	101.3	971.3	9.48
6	0.00	0.00	0.00	0.00	0.00	10.00	15.0	101.3	-194.2	0.37
7	0.00	0.00	0.00	10.00	0.00	0.00	372.6	1013.3	122.2	1.09
8	0.00	0.00	0.00	0.00	2.65	0.00	15.0	101.3	13.0	0.31
9	0.00	0.00	0.00	0.00	2.65	0.00	229.3	1013.3	27.6	0.31
RSTIG1	23.23	76.72	0.05	1.64	0.00	0.00	15.0	101.3	294.1	6.87
2	23.23	76.72	0.05	1.64	0.00	0.00	338.7	1013.3	639.6	6.99
3	23.23	76.72	0.05	11.64	0.00	0.00	304.0	1013.3	709.9	8.00
4	23.23	76.72	0.05	11.64	0.00	0.00	609.5	1013.3	1117.5	8.57
5	15.77	76.72	5.18	15.84	0.00	0.00	1200.0	1013.3	2077.8	9.61
6	15.77	76.72	5.18	15.84	0.00	0.00	669.7	101.3	1257.2	9.73
7	15.77	76.72	5.18	15.84	0.00	0.00	383.8	101.3	849.6	9.21
8	15.77	76.72	5.18	15.84	0.00	0.00	188.1	101.3	585.1	8.74
9	0.00	0.00	0.00	0.00	0.00	10.00	15.0	1013.3	-194.2	0.37
10	0.00	0.00	0.00	9.33	0.00	0.67	180.5	1013.3	70.3	0.99
11	0.00	0.00	0.00	0.00	1.87	0.00	15.0	101.3	9.2	0.22
12	0.00	0.00	0.00	0.00	1.87	0.00	229.3	1013.3	19.5	0.22

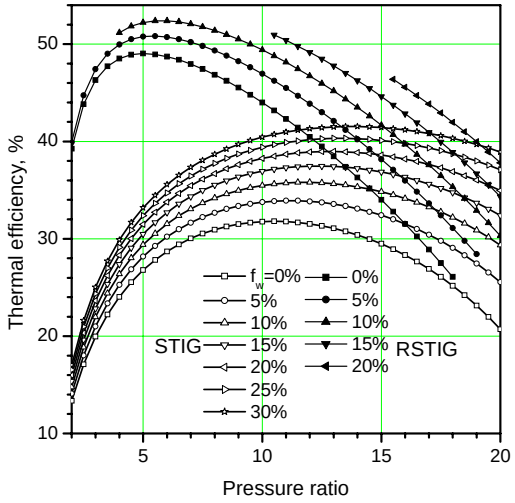

Fig. 2 Thermal efficiency vs. pressure ratio for various steam injection ratios

large pressure ratios or of small pressure ratios and large steam injection ratios. One of the reasons is that as pressure ratio becomes large, the compressor outlet temperature increases while turbine exit temperature decreases so that the temperature difference of the recuperator decreases to reach the minimum temperature limit of the heat exchanger. The other one is that when steam injection ratio becomes large, temperature difference in HRSG reaches the pinch point even though temperature difference at inlet or exit of HRSG is quite big.

In Fig. 3, the fuel consumption which is defined as mass flow rate of fuel per unit mass of dry air is plotted against pressure ratio for various steam injection ratio. As pressure ratio increases, the fuel consumption in STIG decreases. However in RSTIG the fuel consumption increases with increasing pressure ratio. In STIG, compressor outlet temperature increases with increasing pressure ratio. The necessary quantity of fuel for the fixed TIT is reduced, so fuel consumption decreases. But in RSTIG as pressure ratio increases, heat recovery by the recuperator is reduced significantly and air temperature entering into the combustor decreases, so fuel consumption decreases. In each system fuel consumption increases with steam injection ratio because of the increase of mass flow rate in the combustor.

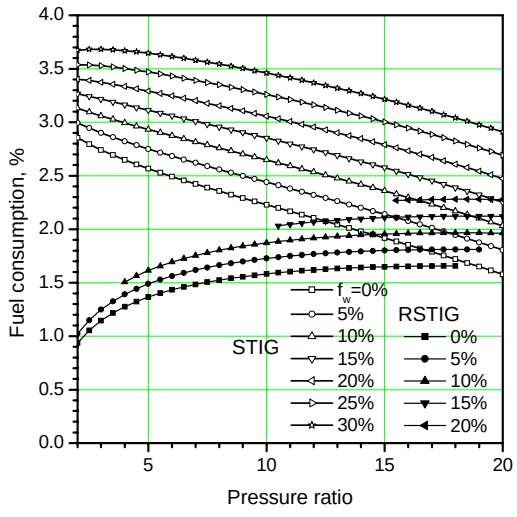

Fig. 3 Fuel consumption vs. pressure ratio for various steam injection ratios

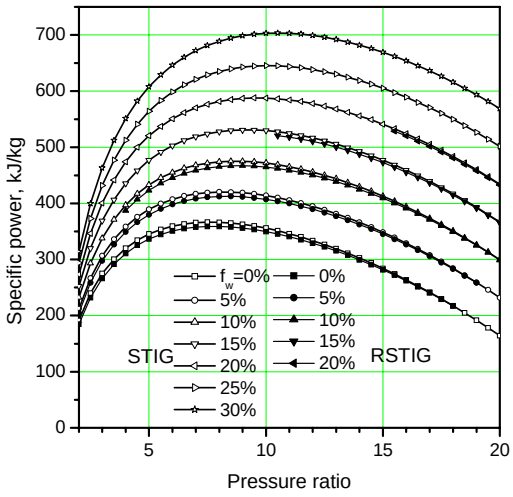

Fig. 4 Specific power vs. pressure ratio for various steam injection ratios

In Fig. 4, the specific power is plotted versus the pressure ratio for various steam injection ratio. In each system, the specific power which is defined as net work per unit mass of dry air shows a maximum value along pressure ratio. The specific power in RSTIG is a little smaller than that in STIG. For a given pressure ratio, specific power increases with increasing of steam injection ratio in each system because the mass flow rate in turbine increases whereas that in compressor is fixed. Figure 5 shows thermal efficiency as a function of specific power. It can be seen that the pressure ratio for maximum specific power is a little bigger than that for the maximum thermal efficiency, which would have an advantage in operating a gas turbine system.

As of the previous mentions, the thermal efficiency is

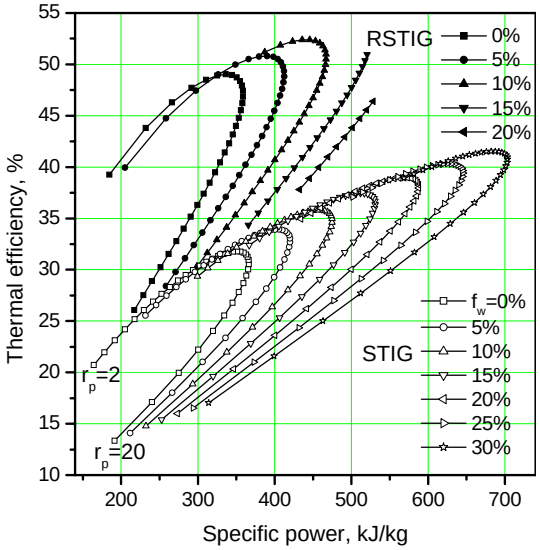

Fig. 5 Thermal efficiency vs. specific power for various steam injection ratios and pressure ratio

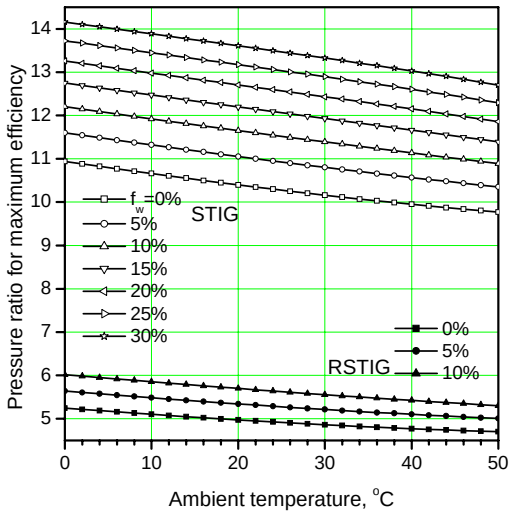

Fig. 6 Pressure ratio vs. ambient temperature for various steam injection ratios

known to have a maximum value along pressure ratio. The effects of ambient temperature and steam injection ratio on the optimum pressure ratio are shown in Figure 6. The result shows that the optimum pressure ratio in RSTIG is greater than that in STIG and decreases linearly with respect to ambient temperature and increases also with increasing of steam injection ratio in each system. Effects of ambient temperature on the maximum thermal efficiency are shown in Fig. 7. The maximum thermal efficiency of RSTIG is greater than that of STIG and decreases monotonically with respect to ambient temperature. It increases with steam injection ratio in each system.

Figure 8 shows the effects of ambient temperature on fuel consumption under the conditions of the maximum thermal efficiency. In each system fuel consumption increases with ambient temperature and its increasing rate is getting greater as ambient temperature becomes higher, and increases with increase of steam injection ratio. The effects of the ambient temperature on the specific power are shown in Fig. 9 under the conditions of the maximum thermal efficiency. In each system specific power has a minimum value, and the specific power in RSTIG is less a little than that of STIG. However, the variation of specific power due to ambient temperature is not significant. For a given ambient temperature, the specific power increases with increasing steam injection ratio in each system. Figure 10 shows the characteristics of maximum thermal efficiency as a function of specific power. It can be said that effects of steam injection ratio are more significant than those of ambient temperature on the maximum thermal efficiency.

Figure 11 shows the effects of TIT on the optimum pressure ratio. It is shown that the optimum pressure ratio increases linearly with respect to TIT and increases with increasing of steam injection ratio in each system. The maximum thermal efficiency is plotted versus TIT in Fig. 12. The maximum

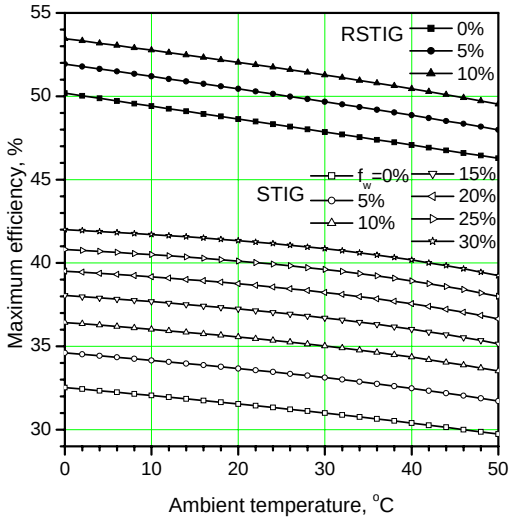

Fig. 7 Maximum thermal efficiency vs. ambient temperature for various steam injection ratios

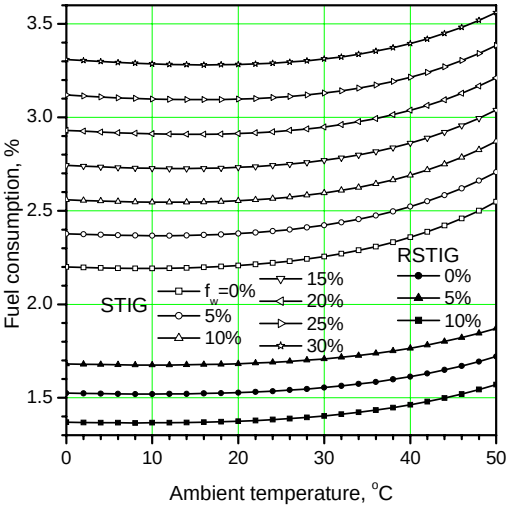

Fig. 8 Fuel consumption vs. ambient temperature for various steam injection ratios

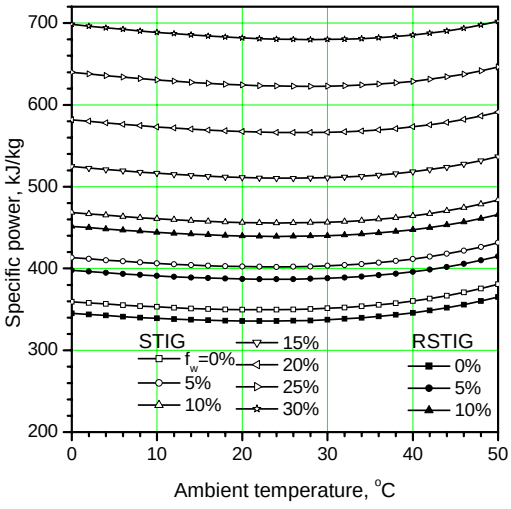

Fig. 9 Specific power vs. ambient temperature for various steam injection ratios

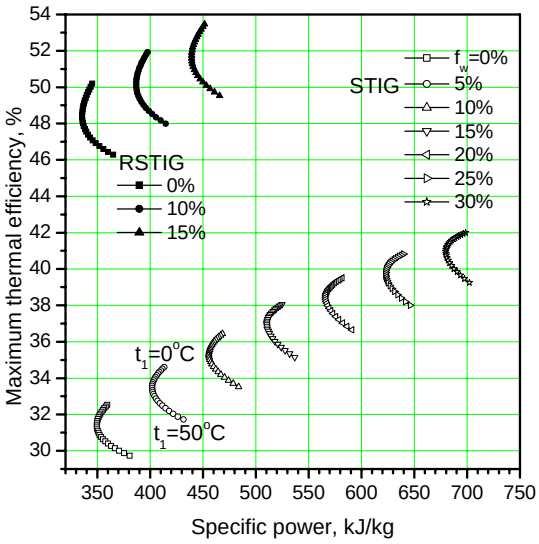

Fig. 10 Maximum thermal efficiency vs. specific power for various steam injection ratios and ambient temperature

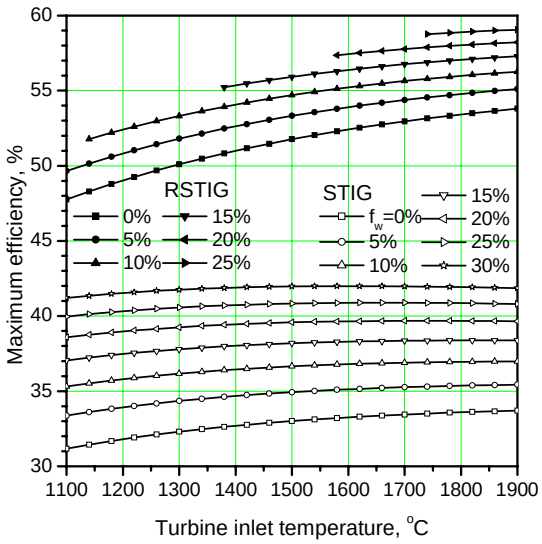

Fig. 12 Maximum thermal efficiency vs. TIT for various steam injection ratios

thermal efficiency in each system increases with increasing TIT or steam injection ratio monotonically. However its increasing rate is reduced as TIT or steam injection ratio increases. The increasing rates for RSTIG are greater than those of STIG. Figure 13 shows variation of the fuel consumption under the conditions of the maximum thermal efficiency. Fuel consumption in each system increases with increasing TIT or steam injection ratio. In Fig. 14, the specific power is plotted against TIT for various steam injection ratio. In each system as TIT or steam injection ratio increases, the specific power increases monotonically. In Fig. 15 the maximum thermal efficiency is shown. It is noted that effects of TIT in RSTIG are more significant than those in STIG.

IV. Conclusions

In this paper, the performance characteristics of the STIG and RSTIG systems have been thermodynamically analyzed. The main results are as follows.

- In both STIG and RSTIG systems the thermal efficiency or specific power has a maximum value with respect to pressure ratio, and increases significantly with increasing steam injection ratio. In RSTIG, it may not be possible to operate in the range of large pressure ratios or of small pressure ratios and large steam injection ratios.
- Fuel consumption per unit mass of dry air in STIG decreases whereas that in RSTIG increases with pressure ratio. However, the fuel consumption increases with steam

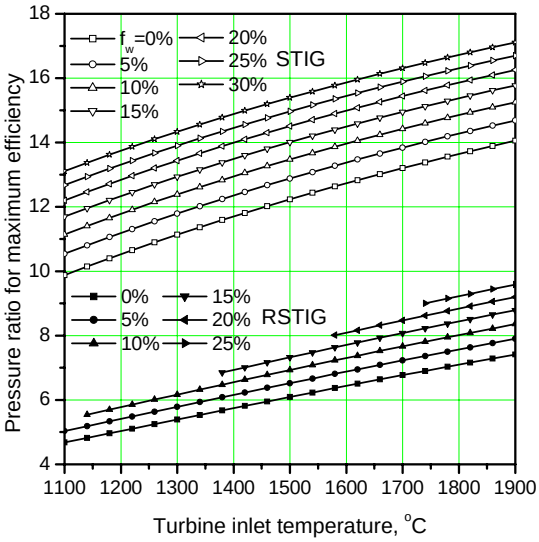

Fig. 11 Pressure ratio vs. TIT for various steam injection ratios

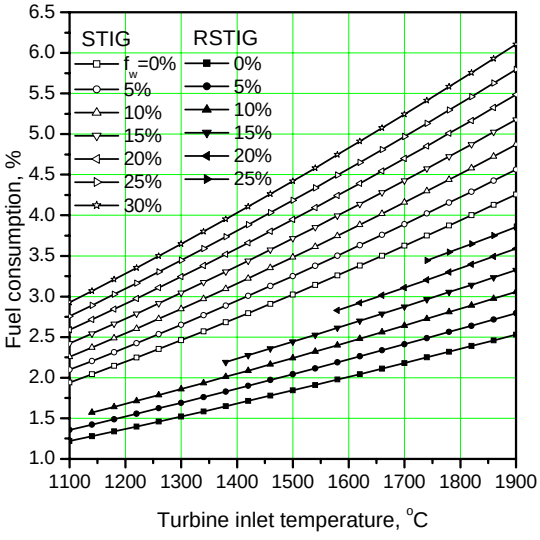

Fig. 13 Fuel consumption vs. TIT for various steam injection ratios

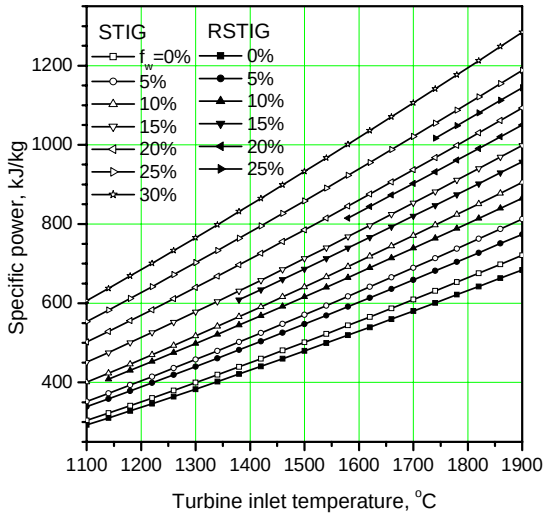

Fig. 14 Specific power vs. TIT for various steam injection ratios

injection ratio in each system.

- In each system the maximum thermal efficiency or the optimum pressure ratio decreases with increasing ambient temperature and increases with increasing steam injection ratio or TIT. The maximum efficiency in RSTIG is greater than that in STIG. However the optimum pressure ratio in

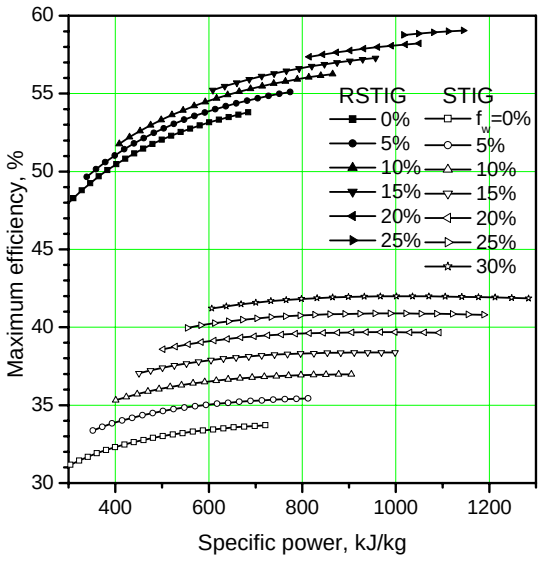

Fig. 15 Maximum thermal efficiency vs. specific power for various steam injection ratios

RSTIG is smaller than that in STIG.

- In each system the specific power under the condition of maximum efficiency has a minimum value with respect to ambient temperature. However, the variation of specific power is negligible. The specific power increases noticeably with increasing the injection ratio or TIT.

ACKNOWLEDGMENT

This research was supported by Basic Science Research Program through the National Research Foundation of Korea (NRF) funded by the Ministry of Education, Science and Technology (No. 2010-0007355).

REFERENCES

[1] M. Lior, Advanced energy conversion to power, Energy Convers Mgmt 38(1997) 941-55.
[2] M. Jonsson, J. Yan, Humidified gas turbines - a review of proposed and implemented cycles, Energy 30(2005) 1013-1078.
[3] A. Poullikkas, An overview of current and future sustainable gas turbine technologies, Renewable and Sustainable Energy Reviews 9(2005) 409-443.
[4] M. Chaker, C.B. Meher-Homji, T. Mee III, Inlet fogging of gas turbine engines - Part I: Fog droplet thermodynamics, heat transfer and practical considerations, ASME J. of Eng for Gas Turbines and Power 126(2004) 545-558.
[5] R. Bhargava, C.B. Meher-Homji, Parametric analysis of existing gas turbines with inlet evaporative and overspray fogging, J. of Engineering for Gas Turbines and Power 127(2005) 145-158.
[6] A.J. White, A.J. Meacock, An evaluation of the effects of water injection on compressor performance, ASME paper No. 2003-GT-38237, and ASME J. of Eng. Gas Turbines and Power 126(2004) 748-754.
[7] K.H. Kim, H. Perez-Blanco, An Assessment of high-fogging potential for enhanced compressor performance, ASME paper No. GT2006-90482, Barcelona.
[8] H. Perez-Blanco, K.H. Kim, S. Ream, Evaporatively-cooled compression using a high-pressure refrigerant, Appl Energy 84(2007) 1028-1043.
[9] K.H. Kim, H. Perez-Blanco, Potential of regenerative gas-turbine systems with high fogging compression, Appl En-ergy 84(2007) 16-28.
[10] K.H. Kim, H.J. Ko, H. Perez-Blanco, Exergy analysis of gas-turbine systems with high fogging compression, Int. J. Exergy (2010), to be published
[11] F.J. Wang, J.S. Chiou, Integration of steam injection and inlet air cooling for a gas turbine generation system, Ener-gy Convrs Mgmt 45(2004) 15-26.
[12] A.M. Bassily, Effects of evaporative inlet and aftercooling on the recuperated gas turbine cycle, Appl Therm Eng 21(2001) 1875-1890.
[13] K. Nishida, T. Takaki, S. Kinoshita, Regenerative steam-injection gas-turbine systems, Appl Energy 81(2005) 231-246.
[14] D.G. Wilson, The design of high-efficiency turbo-machinery and gas turbines, MIT press, Ch. 3, 1984.
[15] Y.A. Cengel, M.A. Boles, Thermo- dynamics. An engineering approach, 5th Ed, McGraw-Hill, 2006.
[16] Y.A. Cengel, Heat and mass transfer. A practical approach, 3rd Ed, Mc Graw-Hill, 2006.